Construction and Building Materials 495 (2025) 143533

Contents lists available at ScienceDirect

Construction and Building Materials

journal homepage: www.elsevier.com/locate/conbuildmat

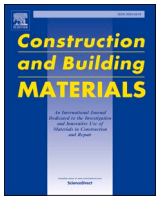

Enhancing properties of cement mortar with tyre-char derived graphene oxide: Mechanical and microstructural analysis

Weeraddhana Chethana Himeshani Silva [a], Tuan Ngo [b], Rabin Tuladhar [a,c], Mohan V. Jacob [a,*]

[a] Microwave Pyrolysis Lab, College of Science and Engineering, James Cook University, Townsville, QLD 4811, Australia
[b] Department of Infrastructure Engineering, The University of Melbourne, Grattan Street, Parkville, VIC 3010, Australia
[c] School of Engineering and Technology, CQ University, QLD 4701, Australia

ARTICLE INFO

Keywords:
Tyre-char
Graphene Oxide
Cement mortar
Mechanical Properties
Microstructure

ABSTRACT

Cement is one of the most widely used materials in the building industry due to its cost-effectiveness and availability. However, its performance limitations have prompted the incorporation of nanomaterials to improve mechanical and microstructural characteristics. Graphene oxide (GO) has shown significant potential as an additive, though its high-cost limits large-scale application. This study presents a sustainable approach to synthesise GO from waste tyre rubber using microwave-assisted pyrolysis (MAP), followed by characterisation through XRD, Raman spectroscopy, XPS, and SEM. The resulting tyre char-based GO (TC-GO) was incorporated into cement mortar at 0.01 %, 0.03 %, and 0.05 % by weight. For comparison, control samples and samples with only tyre char (TC) were also prepared. The results showed that workability decreased in both TC and TC-GO mixes due to particle agglomeration. Nevertheless, the addition of TC-GO had a greater positive effect on mechanical performance. At 28 days, the highest compressive strengths were reached by 0.01 % TC (29.0 MPa) and 0.03 % TC-GO (30.0 MPa), while the highest flexural strengths were found for 0.03 % TC (6.9 MPa) and 0.03 % TC-GO (7.6 MPa). The 0.03 % TC-GO sample performed the best overall, with a 15 % improvement in both strengths over the control. SEM and EDS analyses confirmed a denser microstructure and a reduced Ca/Si ratio (1.9 vs. 2.4 in control), indicating enhanced calcium silicate hydrate (C-S-H) formation. These findings highlight the potential of TC-GO as a low-cost, sustainable nanomaterial for improving the durability and mechanical performance of cement mortar.

1. Introduction

Cement composites are widely used in the construction industry due to their cost-effectiveness and the abundant availability of raw materials. However, their practical applications are limited by their inherent quasi-brittle behaviour, which results in fracture propagation and low tensile strength [1]. To address these limitations and improve performance, various additives has been added into cement matrices. Among these, graphene oxide (GO) has emerged as a promising nanomaterial [2]. GO is a graphene derivative made of a single layer carbon sheet functionalised with oxygen groups such as hydroxyl, carboxyl, and epoxy. These oxygen functional groups can interact with calcium ions released during cement hydration, facilitating nucleation and growth of calcium silicate hydrate (C-S-H) gels [3]. This interaction leads to a more refined and interconnected microstructure. As a result, GO enhances the mechanical properties, durability, and resistance to microcrack formation in cement composites [4].

A common approach for synthesising GO involves the oxidation of natural or synthetic graphite using strong oxidising agents, followed by exfoliation through ultrasonication [5]. However, use of both natural and synthetic graphite as precursors presents several challenges. Natural graphite is geographically limited, and the production of synthetic graphite requires extremely high temperatures ($\geq$ 2500 °C), resulting in substantial energy consumption and high production costs [6]. In contrast, carbon-rich residues and biomass waste have emerged as attractive alternatives for synthesising graphene-based materials, including GO. These sources offer several advantages, including high carbon content, environment-friendliness, lower processing temperature, wide availability, and cost-effectiveness [7]. Numerous studies [8] have investigated the utilisation of different carbon precursors and biomass, such as coconut shells [9], sugarcane bagasse [10], tea [11], pine leaves [12], oil palm leaves [13], and industrial wastes including

* Corresponding author.
E-mail address: mohan.jacob@jcu.edu.au (M.V. Jacob).

https://doi.org/10.1016/j.conbuildmat.2025.143533
Received 14 March 2025; Received in revised form 28 July 2025; Accepted 5 September 2025
Available online 17 September 2025

scrap tyres [14], bio-soot [15], and Zn-C batteries [16], for GO synthesis.

Among industrial wastes, scrap tyres have become a significant global environmental concern. It was estimated that 1.0 billion tyres are produced worldwide annually [17]. Every year, millions of discarded tyres are either thrown away or buried, posing severe risks to the environment, the economy, and public health. By 2030, the number of discarded tyres is expected to reach 1.2 billion [18]. Recent research has focused on developing recycling methods for waste tyres. One promising approach is the pyrolysis of waste tyres, which allows for energy recovery and the production of reusable materials. There are different pyrolysis processes for the treatment of the waste tyres including vacuum, microwave, catalytic and co-pyrolysis [19]. Among these, microwave-assisted pyrolysis (MAP) is particularly effective for processing waste tyres. This is because, the reinforcing carbon black in the tyre rubber, a material with low thermal conductivity, can improve the absorption of microwave energy within the rubber. This, in turn, promotes the pyrolysis of the rubber and leads to increased tyre char (TC) production. [19]. Compared to the traditional pyrolysis, MPA reduced processing time and energy consumption while offering a more environmentally friendly and cost-effective solution for waste tyre treatment [19].

GO demonstrates exceptional performance in cement applications by enhancing the mechanical and microstructural properties. The oxygen functional groups on GO decrease van der Waals forces and enhance electrostatic repulsion between GO sheets, which promotes its dispersion in water. As a result, GO forms stable suspension primarily composed of 1-nm-thick sheets, making it more compatible for integration into cement mixtures [4]. Additionally, these functional groups play a key role in physical or chemical interactions, enhancing the interfacial bonding and overall composite performance [20]. GO-enhanced cement is suitable for different applications such as for high-traffic areas like roads, pavements, and bridges due to its high strength, durability and abrasion resistance [21].

However, the high cost of commercial GO poses challenges for its widespread application. Most existing studies focus primarily on GO synthesis from graphite and its effects on cement paste and mortar. In contrast, this study investigates the synthesis of GO from TC and its impact on cement performance. To the best of our knowledge, this is the first study to report the synthesis of GO from TC and its application in cement. In this study, GO was synthesised from TC using the MAP method, using a two-phase microwave power system with two stages, followed by chemical treatments with $FeCl_3$ and H_2SO_4. Typically, GO is incorporated into cement composites in the range of 0.01–0.1 wt% by weight of cement (bwoc), as higher dosages may lead to agglomeration and reduced effectiveness. Reported improvements in compressive strength range from 10 % to 40 %, while flexural strength can increase by 15–60 %, depending on mix design, curing conditions, and dispersion techniques [4]. TC-derived GO (TC-GO) was incorporated into cement at concentrations of 0.01 %, 0.03 %, and 0.05 % bwoc to assess its effects on workability, compressive strength, and flexural strength and to compare these results with previous studies. Control samples and those containing only TC were also prepared and tested for comparison. Additionally, a microstructural analysis was conducted to evaluate the impact of TC-GO on the cement matrix.

2. Experimental investigation

The experimental work was carried out in two stages. The first stage involved the synthesis and characterisation of TC-GO using a two-step MAP process. The second stage focused on the preparation and testing of cement mortar, including assessments of flowability, curing behaviour, compressive and flexural strength and microstructural properties.

2.1. Synthesis of graphene oxide from tyre char

The synthesis of TC-GO was performed in two steps using a MAP technique, as detailed in our recent work [22]. In the first step, waste tyre rubber was converted into TC and in the second step, the TC was chemically treated and further processed via MAP to produce TC-GO. Fig. 1 shows both the real-world MAP system and schematic diagram used in this study. As shown in Fig. 1(b), the system includes a nitrogen gas (N_2) flow controller (a), a feedstock chamber (b), a manual tuner (c), a microwave generator (d) a control unit (e), a water chiller (f), condensers (h) for collecting liquid by-products (g), and a vacuum pump (i) that maintains a negative pressure of 50–80 kPa.

2.1.1. Chemicals and materials

The materials used in this research included scrap tyres supplied by Mycar Tyre & Auto, Townsville. Ferric Chloride ($FeCl_3$), Sulfuric acid (H_2SO_4, 95 %), Hydrochloric acid (HCl, 95 %) and ethanol (C_2H_5OH, 95 %) were purchased from Sigma-Aldrich, Australia. All the chemicals were used as received.

2.1.2. Preparation and characterisation of TC-GO

The scrap tyres were cleaned and cut into small square pieces (1 cm × 1 cm). Approximately 100 g of these fragments were processed in a microwave pyrolysis process. The tyre pieces were exposed to two microwave power phases: first 0.8 kW for 15 min, followed by 1.0 kW for 45 min, for a total of one hour of pyrolysis. The resulting TC treated with diluted HCl acid to eliminate contaminants and washed with distilled H_2O until the pH reached 7. Then the obtained TC sample was oven dried at 105 °C. To prepare a suspension, the dried TC was mixed with $FeCl_3$ in distilled water at a 1:1 ratio. After 10 min of sonication, the solution was evaporated at 80 °C in an oven for 24 h. The produced black solid was then subjected to a second microwave pyrolysis procedure at 0.8 kW for 15 min, followed by 1.0 kW for 30 min, for a total of 45 min of pyrolysis. The obtained sample was then rinsed with diluted HCl and distilled water before being treated with H_2SO_4. After treatment of conc. H_2SO_4, the resulting product was oven-dried to produce TC-GO and further analysed. The synthesis steps of TC-GO from scrap tyres are illustrated in Fig. 2.

The crystal structure and interlayer spacing of the synthesised TC-GO were analysed using a Bruker D2 Phaser X-ray diffractometer, scanned over a 2θ range from 5° to 80° at 8° /min. Interlayer spacing was calculated using Bragg equation: $2d\sin\theta = n\lambda$, and crystallite size was estimated using the Debye-Scherrer equation: $n\lambda/\beta\cos\theta$, where λ stands for the X-ray wavelength, θ is the scattering angle, β is the full width at half maximum (FWHM), and n is the diffraction order. Raman spectroscopy was performed at room temperature using a WITec Raman spectrometer with a 532 nm laser, scanning across 100–4000 cm^{-1} . The sample was sonicated in ethanol and drop-cast onto a silicon wafer prior to analysis.

X-ray photoelectron spectroscopy (XPS) was conducted using a Kratos Axis Ultra system with an Al Kα X-ray source. Binding energies were calibrated against the C 1 s peak at 284.8 eV from incidental carbon. Surface microstructure analysis was conducted using a Hitachi SU 5000 scanning electron microscope (SEM) at an accelerating voltage of 1.5 kV. Samples were coated with a thin platinum layer via spray coating prior to imaging. The Energy Dispersive X-ray Spectroscopy (EDS) analysis was carried out using an Oxford Instruments X-MaxN EDS detector. EDS analysis was conducted using both point scans and a selected area scan to evaluate the elemental composition across different features of the sample.

2.2. Preparation of cement mortar

The prepared TC-GO was incorporated into the cement to investigate its effects on mechanical strength and microstructural properties. For comparison, both control and TC cement mortars were also prepared.

2.2.1. Chemicals and materials

General-purpose (GP) cement was used in this investigation to

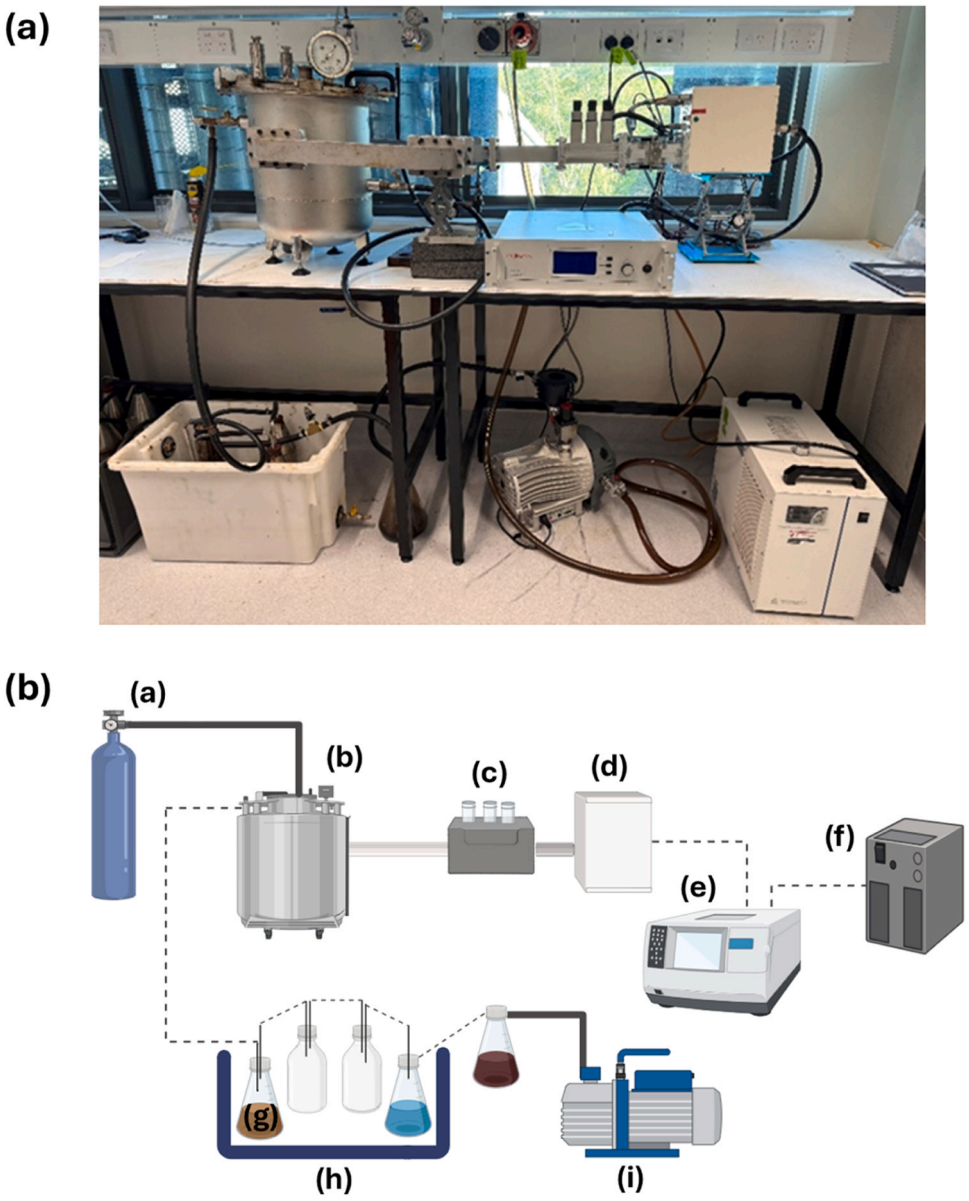

Fig. 1. The real-world MAP system and the sketch diagram [22]: (a) N_2 cylinder; (b) Feedstock chamber; (c) Manual tuner; (d) Microwave generator; (e) Microwave controller; (f) Water chillier; (g) Oil collector; (h) Condensers; (i) Vacuum pump.

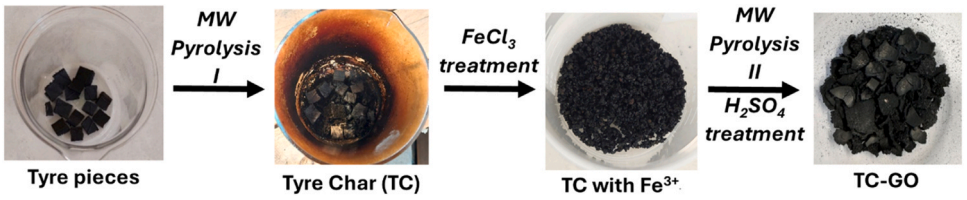

Fig. 2. The synthesis steps of TC-GO from tyre rubber.

Table 1
Chemical composition of GP cement used in the study.

Material	Chemical Composition (wt%)									
	CaO	SiO_2	Al_2O_3	Fe_2O_3	SO_3	MgO	K_2O	TiO_2	Na_2O	LOI
%	64.8	20.7	6.0	3.3	2.8	1.4	0.5	0.3	0.2	2.7

adhere to the specifications outlined in AS 3972–2010 [23]. The chemical composition of the GP cement is presented in Table 1. River sand was used as a fine aggregate. TC and TC-GO synthesised as described in Section 2.1 were used in this study. A polycarboxylic ether-based MasterGlenium SKY 8100 superplasticiser produced by Master Builders Solutions Co., Ltd was used for workability.

2.2.2. Preparation of TC and TC-GO water suspension

TC and TC-GO were thoroughly combined with water and superplasticiser before being added into the dry cement materials to improve their dispersion inside the cement matrix. In this study, ultrasonicator (Model FXP10DH) was used to make an aqueous solution. The necessary quantities of TC powder, water, and superplasticiser (PS) were carefully measured. Water was gradually added until the specified water-to-cement (W/C) ratio was obtained. These components were then mixed to create an aqueous solution, which was subsequently dispersed to ensure a uniform distribution. The dispersion was conducted 30 min with a frequency of 40 kHz and a power of 100 W. This procedure was also repeated to prepare TC-GO water suspensions and control samples.

2.2.3. Preparation of TC and TC-GO incorporated cement paste

Cement mixing was conducted after preparing the TC and TC-GO suspensions. A cement mortar mixer (Model 65-L0006/AM) was used to prepare the cement mixture. The mixing procedures similar to AS 2350.12–2006 [24] were followed. According to the cement mix design, the calculated amount of cement was combined with the prepared TC suspension in the mixing bowl. Immediately after adding the cement and suspensions, the mixer was started at a low speed for 30 s. The sand was then gradually added over the next 30 s. The mixer was set to high speed and allowed to run for an extra 30 s. Afterwards, the mixer was stopped for 90 s. Using a scraper, all mortar adhering to the wall and bottom of the bowl was collected in the centre within the first 15 s. The mixing was completed at high speed for 60 s. After mixing, the cement paste mixture was promptly poured into molds (40 × 40 × 160 mm in size) and compacted on a vibrating table. The mould used in determining the compressive and flexural strength was prepared for three specimens. For each trial, three specimens were tested.

The molds were then covered with polyethylene sheets to prevent the mixture from escaping. The cement specimens were demolded after 24 h and stored in a humidity cabinet at 23 °C and 50 % humidity. The samples were then cured in a saturated lime water bath at 20 °C for 7 days and 28 days of testing. This procedure was repeated for preparing TC-GO as well as control samples. Table 2 lists the mixed proportions of the prepared TC and TC-GO cement mortar and paste. The water-to-cement ratio was constant at 0.73 for all the mixtures.

2.2.4. Flow table test

Immediately after mixing, the fresh mixture was tested using a flow table to determine the workability of the cement paste. The flow table was used to determine a flow according to AS 2701.2001 [25]. This test method determines the relative water requirement by assessing the amount of water needed for a specified flow (110 ± 5). Fig. 3 shows the setup for the flow table test. The flow table test was performed to compare the flow and workability of the control cement samples with the TC and TC-GO cement samples, Additionally, the flow test results of TC and TC-GO cement pastes were compared to evaluate their differences.

2.2.5. Mechanical properties

Table 3 presents a comprehensive summary of the testing methods employed in this research to assess the mechanical properties of control, TC, and TC-GO cement mortars. The test results reflect average values calculated from at least three samples, with an allowable deviation of 1 %. Any values exceeding this range were considered outliers. Fig. 4 illustrates the each testing method. The Shimadzu Universal Testing Machine (Model AGS-50kNX) was used for both compressive and flexural tests. The flexural test was executed using a three-point bonding. All tests were conducted after curing periods of 7 and 28 days.

2.2.6. Microstructure characterisation

Following 28-day compression testing, the central portions of the fractured mortar samples were collected and immersed in acetone to halt hydration. Before SEM analysis, these samples were vacuum-dried in an oven at 105 °C for 3 h and then stored in a vacuum chamber until examination. Surface morphology was observed using SEM imaging, while energy-dispersive X-ray spectroscopy (EDS) and elemental mapping were used to investigate the elemental composition and spatial distribution of important elements such as C, O, Si, and Ca in both control and TC-GO mortar samples.

3. Results and discussion

3.1. Characterisation of the prepared TC-GO

The X-ray Diffraction (XRD) pattern of the synthesised TC-GO, shown in Fig. 5 exhibits a strong peak at 9.8° (001), a broad peak at 25° (002), and a weak peak at 43° (100) [15,26]. The prominent peak at 9.8° corresponds to an interlayer spacing of 0.90 nm, indicating the presence of oxygen-containing intercalation groups with the graphitic layers [15]. The broader peak at 25° suggests a persistent poorly crystalline nature of the precursor used for synthesis [9]. The crystallite size of the peak at 9.8° of TC-GO (001) was calculated using Scherrer's equation as 26.09 nm. The XRD pattern of TC-GO shows GO formation with the presence of its amorphous precursor material and a reduced GO phase. The formation of rGO may result from the use of amorphous material and changes in the oxidation degree during the synthesis process.

The Raman spectrum of TC-GO, shown in Fig. 6 exhibits three different bands. Two of them are located at 1344 and 1590 cm^{-1}, corresponding to the D and G, respectively, while three smaller bands, at 2500–3250 cm^{-1} are designated as 2D peaks. The I_D/I_G ratio of 0.99 for TC-GO indicates a higher number of defects, which can be attributed to the attachment of functional groups, such as hydroxyl and epoxy groups, to the carbon skeleton [12].

Fig. 7(a) shows the XPS data, which reveals that TC-GO primarily

Table 2
Mix proportions of cement mortar.

Sample	TC % (bwoc)	TC-GO % (bwoc)	W/C ratio	Cement (g)	TC (g)	TC-GO (g)	Sand (g)	Water (g)	PS (ml)
Control	0.00	0.00	0.73	450	0.000	0.000	1350	329	4.5
TC1	0.01		0.73	450	0.045		1350	329	4.5
TC3	0.03		0.73	450	0.135		1350	329	4.5
TC5	0.05		0.73	450	0.225		1350	329	4.5
TC-GO1		0.01	0.73	450		0.045	1350	329	4.5
TC-GO3		0.03	0.73	450		0.135	1350	329	4.5
TC-GO5		0.05	0.73	450		0.225	1350	329	4.5

*bwoc = by weight of cement
*PS = superplasticiser

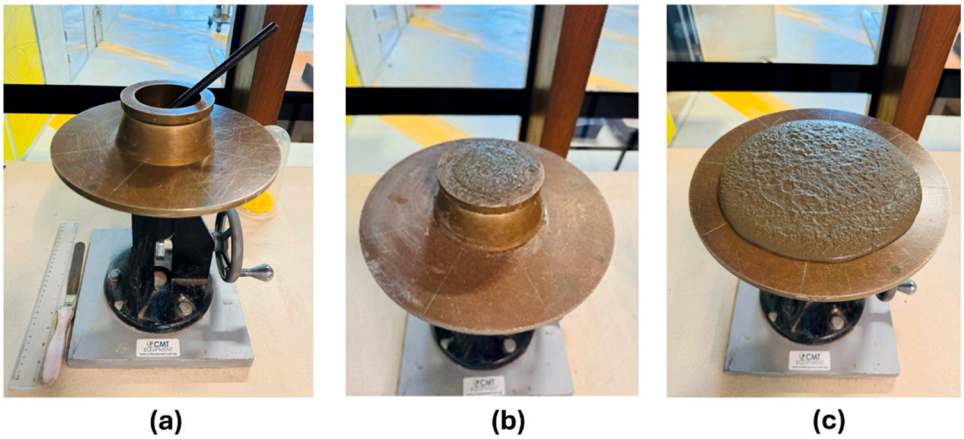

Fig. 3. Flow table test set-up: (a) Flow table with mould with tamper; (b) mould filled with mortar sample; (c) flow measurement after dropping.

Table 3
Mechanical Test methods of cement mortar.

Test parameter	Test standard	Sample type	Sample dimensions	Loading rate (kN/s)
Compressive strength	AS/NZS 2350.11:2006	Prisms	40 × 40 × 160 mm	2.4 ± 0.2
Flexural strength	ASTM C 348–08	Prisms	40 × 40 × 160 mm	2.6 ± 0.1

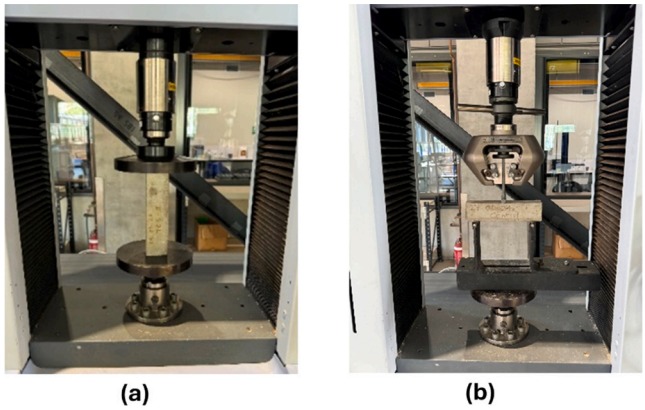

Fig. 4. (a) Compressive strength test set up, (b) Flexural strength test set up.

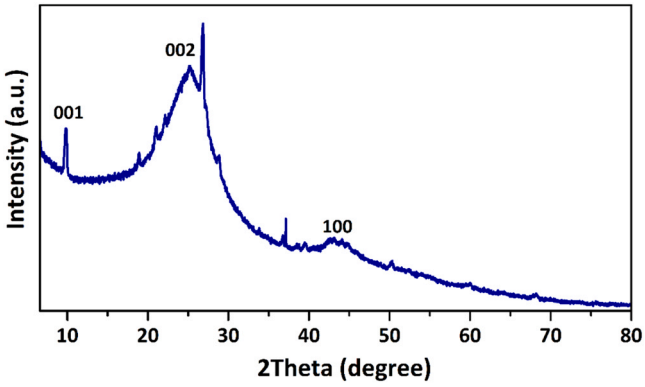

Fig. 5. The XRD pattern of TC-GO.

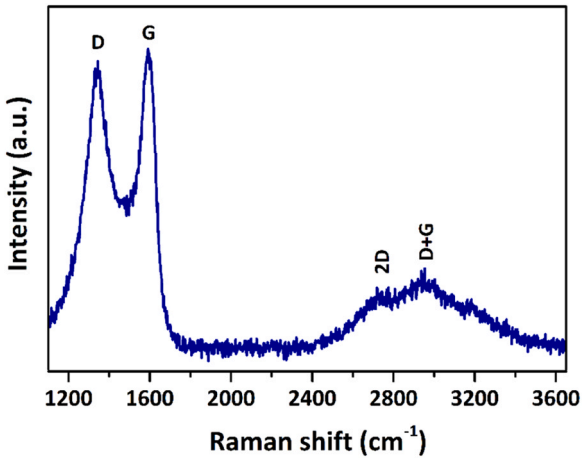

Fig. 6. The Raman spectrum of TC-GO.

consists of C and O, with trace amounts of S and Zn detected as impurities originating from the precursor. The C1 spectrum in Fig. 7(b) indicates four carbon states: sp^2 and sp^3 hybridised carbon, as well as C–O and O–C═O structures [27]. The atomic carbon-to-oxygen (C/O) ratio of TC-GO, as quantified by XPS, is 1.92. This analysis demonstrates a significant increase in the atomic concentration of oxygen-containing groups, such as carbonyl and carboxyl groups, in the TC-GO sample.

SEM images of TC-GO in Fig. 8(a-b) reveal a disordered solid, comprising indistinctly aggregated, thin, closely associated, and highly overlapping sheet structures. The observed wrinkling is attributed to interactions between oxygen-containing functional groups [20]. The EDS analysis of the TC-GO sample, as shown in Fig. 8(c), indicates atomic percentages of 79.69 % for C and 15.89 % for O, with impurities such as S, Fe, and Zn present. The characterisation of GO synthesised from TC confirms a defined interlayer distance, verifying the structure and highlighting some impurities from the original precursors.

Further details of the TC-GO characterisation are provided in our recently published work [22]. In this process, $FeCl_3$ functions both as a mild oxidising agent and a catalyst, enhancing the surface functionality of TC more effectively than other chlorides such as $ZnCl_2$. Additionally, H_2SO_4 facilitates both oxidation and exfoliation. Readers are referred to our previous publication for comprehensive explanation in the mechanism of TC-GO synthesis.

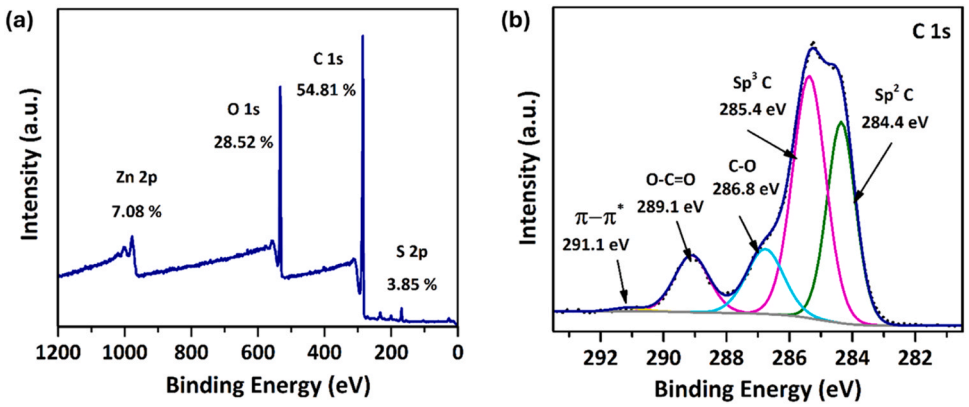

Fig. 7. XPS characterisation of TC-GO (a) XPS survey spectrum (b) C1s spectrum.

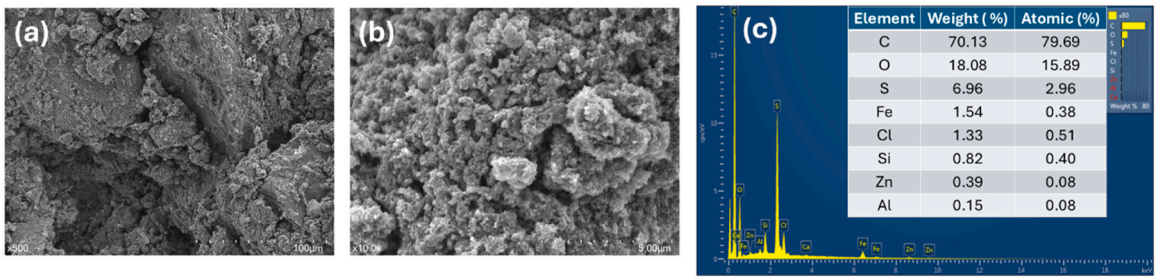

Fig. 8. (a-b) SEM images, (c) EDS analysis of TC-GO.

Table 4
Flow table test results of TC and TC-GO cement paste.

Sample	TC % (bwoc)	TC-GO% (bwoc)	Flow %
Control	0.00	0.00	106.25
TC1	0.01		101.25
TC3	0.03		100.00
TC5	0.05		96.25
TC-GO1		0.01	95.00
TC-GO3		0.03	88.75
TC-GO5		0.05	85.00

*bwoc = by weight of cement

3.2. *Influence of TC and TC-GO incorporation on the workability of cement paste*

The flow table test was used to determine the workability of plain cement paste, as well as TC and TC-GO incorporated cement pastes by measuring their flow. The data for the flow table test are tabulated in Table 4, which indicates flow data for plain cement, and cement mixtures containing TC and TC-GO of 0.01 %, 0.03 %, and 0.05 % by weight of the cement. Fig. 9 shows the graph of the flow table test with dosage and the flow in percentage. The flow of the plain cement sample was within the standard range. The flow percentages of all TC and TC-GO samples were compared to that of the plain cement sample to evaluate their influence on workability.

The flow table results show that the flow percentage reduced with the increase of TC and TC-GO content, compared to the plain cement past. The incorporation of 0.01 % by weight of TC slightly reduced the flow percentage. However, the incorporation of 0.01 % TC-GO showed a sudden decrease. With the further increase of TC and TC-GO content to 0.03 %, TC did not reduce flow diameter significantly, however, TC-GO reduced it slightly. The addition of 0.05 % of TC and TC-GO showed 9 % and 20 % reduction respectively, than that of the plain cement paste. The flow table test results indicated that the incorporation of TC and TC-GO reduced the workability of the cement paste. Moreover, the addition of TC-GO had more impact on the cement paste compared to the TC.

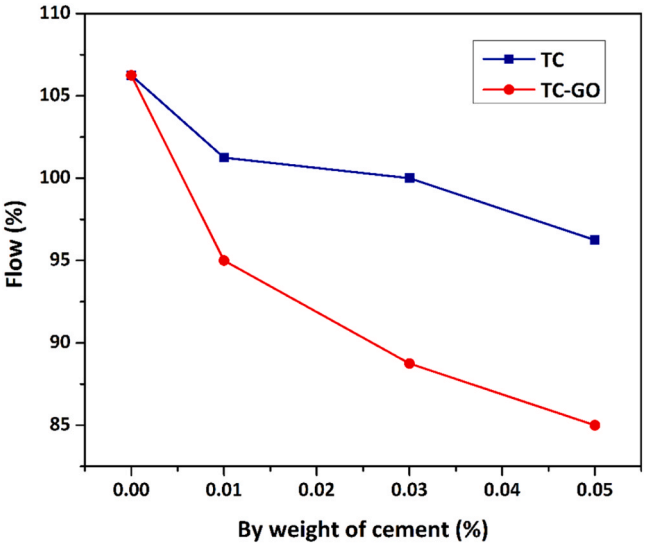

Fig. 9. Flow table test results of TC and TC-GO cement paste.

The results show that 0.03 % is the threshold for maintaining workability in GO-incorporated cement paste. Below this threshold, GO addition significantly reduced workability, while above it, the impact was minimal. Li et al. [28] also found that GO nanosheets lowered the mini-slump values of cement paste. Similarly, Suo et al. [29] observed a marked decrease in fluidity with GO addition. The decrease in workability is attributed to the increased viscosity of the cement matrix caused by the formation of GO agglomerates, which result from chemical cross-linking with calcium ions present in the pore solution of cement paste [30].

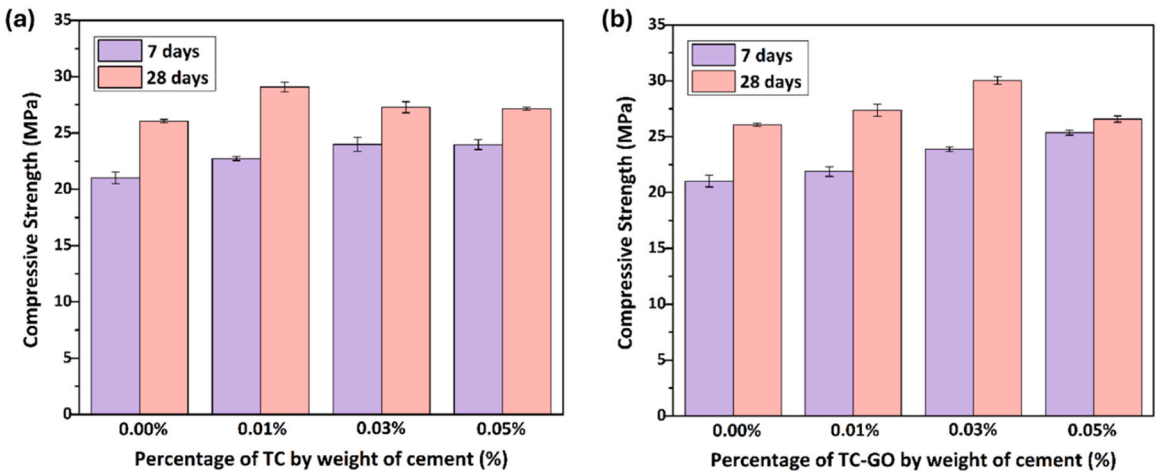

Fig. 10. Compressive strength of (a)TC and (b) TC-GO incorporated cement mortar in 7 and 28 days.

3.3. Mechanical properties of TC and TC-GO cement mortar

Fig. 10 (a) and (b) present the compressive strength results at 7 and 28 days for TC and TC-GO, respectively. In Fig. 10 (a), the compressive strength of the control mix at 7 days is 21.0 MPa, which increases to 26.1 MPa by 28 days. In the 0.01 % TC sample, there is a slight improvement in compressive strength, with the 7-day strength increasing to approximately 22 MPa, and the 28-day strength reaching around 29 MPa. The 0.03 % TC sample shows a 7-day strength of around 24 MPa, while the 28-day strength is slightly higher at 27 MPa. A slight decrease in strength is observed in the 0.05 % TC sample, with values just below 24 MPa at 7 days and slightly above 27 MPa at 28 days.

In Fig. 10 (b), the 7-day compressive strength for the 0.01 % TC-GO sample is similar to the corresponding TC sample at 21.9 MPa, with the 28-day strength reaching above 27 MPa. The 0.03 % TC-GO sample exhibits a 7-day compressive strength of 23.9 MPa, which exceeds 30 MPa at 28 days. The 0.05 % TC-GO sample shows a slight decrease in strength compared to the 0.03 % incorporation, with values around 25 MPa at 7 days and approximately 26 MPa at 28 days. Both TC and TC-GO improve the compressive strength of cement, with 0.03 % TC-GO exhibiting the best overall performance. However, both graphs indicate a slight reduction in compressive strength at the 0.05 % dosage for both 7-day and 28-day curing periods, suggesting that excessive addition of either material may hinder cement performance. This is because of excessive addition of TC and TC-GO can hinder cement performance by increasing water demand, leading to reduced workability and improper hydration. High dosages may cause particle agglomeration, disrupting the cement matrix and introducing porosity, which weakens mechanical properties. Additionally, excessive TC and TC-GO can interfere with hydration reactions, affecting the strength development. A optimal dosage is essential to balance workability and performance.

The increment in compressive strength of TC and TC-GO added cement mortar, compared to the control mix is illustrated in Fig. 11. At 7 days, the compressive strength increment of TC increases and remains relatively stable across the cement weight percentages from 0.01 % to 0.05 %. The value starts at around 8 %, slightly increases near 0.03 %, and stays almost constant at around 14 % from 0.03 % onward. In contrast, the opposite pattern is observed at 28 days. TC at 28 days shows a decreasing trend as the weight of TC increases in the cement mixture It starts at about 11 % for 0.01 %, then drops to just over 5 % at 0.05 %, suggesting a reduction in compressive strength increment over time at higher cement weights.

For TC-GO cement mortar at 7 days, the strength exhibits a steadily increasing trend, starting at 4 % for 0.01 %, and reaching almost 20 % by 0.05 %. However, in TC-GO at 28 days, the strength initially increases sharply to about 15 % at 0.03 %, before dropping dramatically

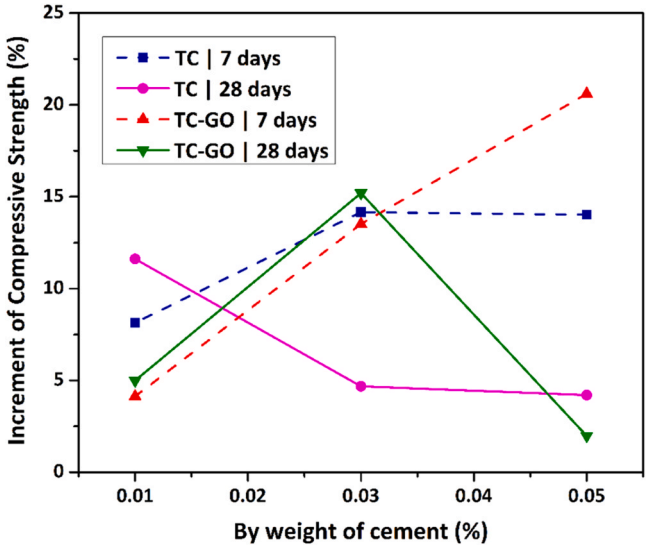

Fig. 11. Compressive strength increment of TC and TC-GO added cement mortar in 7 and 28 days.

to around 2 % at 0.05 %. This suggests that, at 7 days, the incorporation of TC-GO enhances compressive strength over time. However, at 28 days, the strength enhancement diminishes significantly beyond a certain cement weight percentage.

Fig. 12 (a) and (b) present the test results for flexural strength at 28 days for TC and TC-GO respectively. At 28 days, the control mix exhibits a flexural strength of approximately 6.60 MPa. The mixtures with 0.01 % and 0.05 % TC show slightly lower flexural strength values compared to the control, while the mixture with 0.03 % TC achieves a higher flexural strength, reaching around 6.9 MPa, surpassing the control sample. In contrast, the TC-GO incorporated cement mortar displays an increasing trend, with a flexural strength of 7.6 MPa at 0.03 % dosage, surpassing both the control and TC-only mixtures. However, at 0.05 % TC-GO, the flexural strength decreases again, indicating that the optimal dosage lies around 0.03 %.

The increment in flexural strength of TC and TC-GO added cement mortar, compared to the control mix is illustrated in Fig. 13. The 0.01 % dosage of TC experiences around a 4 % decrease in flexural strength while 0.03 % TC shows a 5 % increase in flexural strength compared to the control. A significant 9 % decrease is recorded for the 0.05 % TC sample, which that shows higher percentages of TC lead to a decline in flexural strength. The 0.01 % TC-GO results in a 5 % increase in flexural

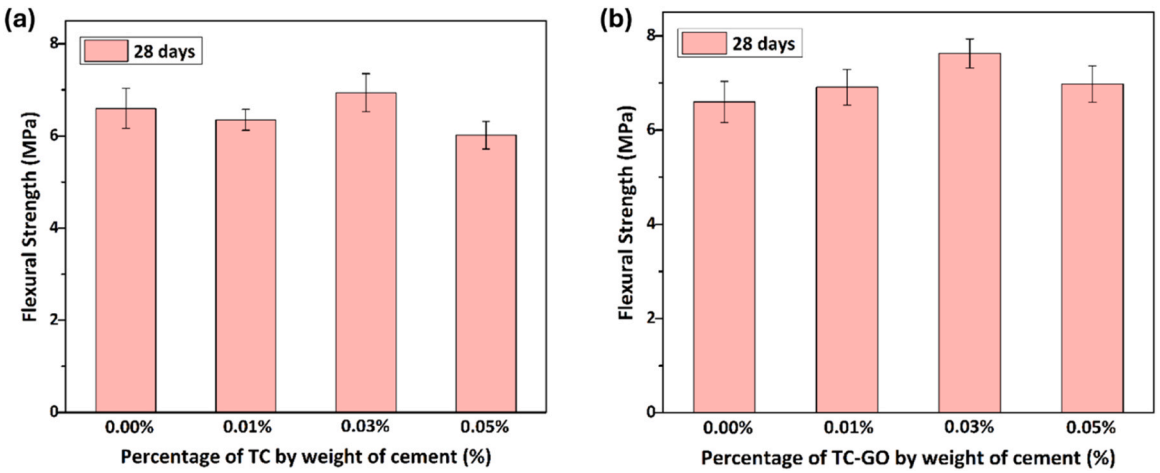

Fig. 12. Flexural strength of (a) TC and (b) TC-GO incorporated cement mortar in 28 days.

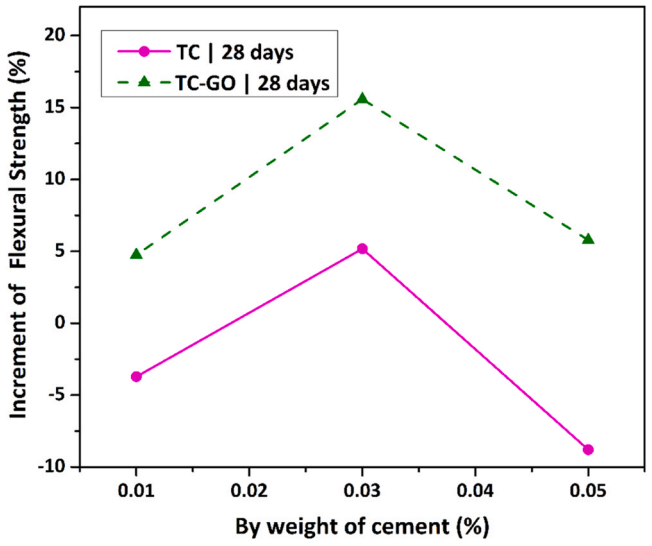

Fig. 13. Flexural strength increment of TC and TC-GO added cement mortar in 28 days.

strength, which is an improvement over the control and TC 0.01 %. The largest increment is exhibited in 0.03 % TC-GO, with a 16 % increase. This indicates that 0.03 % TC-GO is the most effective dosage for enhancing flexural strength. A 0.05 % TC-GO still shows an improvement, with a 6 % increase, though not as significant as at 0.03 %. The optimal dosage for improving flexural strength is 0.03 % for both TC and TC-GO, with TC-GO providing the highest overall improvement. However, at higher percentages (0.05 %), both TC and TC-GO mixtures tend to show a reduction in performance compared to the 0.03 % dosage.

In comparison to the control sample, mechanical strength results showed that adding 0.03 % of TC-GO to cement mortar improved both compressive and flexural strength by 15 % after 28 days. This performance also exceeded that of mortar containing 0.03 % TC. It is highlighted the superior reinforcing capability of the GO structure derived from waste tyre sources. By contrast, Wang et al. [31] reported that the inclusion of 0.03 % GO nanosheets enhanced compressive and flexural strengths by 21.4 % and 39.6 %, respectively. Ullah et al. [32] who evaluated GO 0.01, 0.02 and 0.05 %, found that 0.05 % GO produced the greatest strength enhancements, with compressive and flexural increases of up to 57 % and 48 %, respectively. Similarly, Cui et al.[33] investigated GO dosages of 0.03, 0.06 and 0.09 % and reported strength enhancements ranging from 4.37 % to 9.82 % in compressive strength and 7.78–22.33 % in flexural strength, with 0.06 wt% GO identified as the optimum dosage. Although the strength increases shown in the current study are modest in comparision to those acquired with higher GO concentrations, they are important given the sustainable origin of TC-GO and its effective performance at low doages.

3.4. Influence mechanism of TC and TC-GO on cement hydration products

Incorporating TC-GO into cement mortar improves compressive and flexural strengths by influencing the cement hydration process. Fig. 14 shows the schematic representation of the influence mechanism of TC and TC-GO on the formation of cement hydration products. During the induction phase of hydration, tricalcium silicate (C_3S), the primary component of cement, reacts with water to release calcium ions (Ca^{2+}), essential for forming hydration products [34]. TC-GO can dissolve more Ca^{2+} and direct more Ca^{2+} to the outer layer to produce outer hydration products (OP). This dissolution of Ca^{2+} leads to an accelerated hydration rate during the induction period compared to the control sample, as evidenced by the enhanced mechanical performance [6].

The large surface area of TC-GO offers additional nucleation sites for hydration products like calcium silicate hydrate (C-S-H) and calcium hydroxide (portalandite / $[Ca(OH)_2]$, accelerating hydration and resulting in a denser microstructure compared to TC mortars. Ca^{2+} ions from the C-S-H structure bond with oxygen functional groups on TC-GO sheets, forming a more interconnected network. This intercalation effect densifies the C-S-H gel, enhancing both compressive and flexural strengths in TC-GO cement mortars [35].

According to the classical interpretation of cement hydration [34], C-S-H gel forms in two phases: the outer product (OP) and the inner product (IP). The OP forms around unhydrated cement particles (C) and typically has a higher Ca/Si ratio, making it more porous and less mechanically robust. In contrast, the IP, with a lower Ca/Si ratio, is denser and stronger. Under compressive loads, cracks propagate through both IP and OP, contributing to compressive strength. However, flexural cracks mainly propagate through the OP, making it a key factor in determining flexural strength [6].

The role of TC-GO in improving the mechanical properties can be attributed to its ability to increase the thickness and density of both the IP and OP. As observed, the optimal TC-GO dosage of 0.03 % results in the greatest enhancement in both compressive and flexural strength. At this dosage, the increased thickness of the IP, combined with the improved pore-filling effect of the OP, contributes to the overall densification of the microstructure. This balance between IP and OP leads to superior strength performance at 28 days.

On the other hand, TC samples exhibit a different hydration

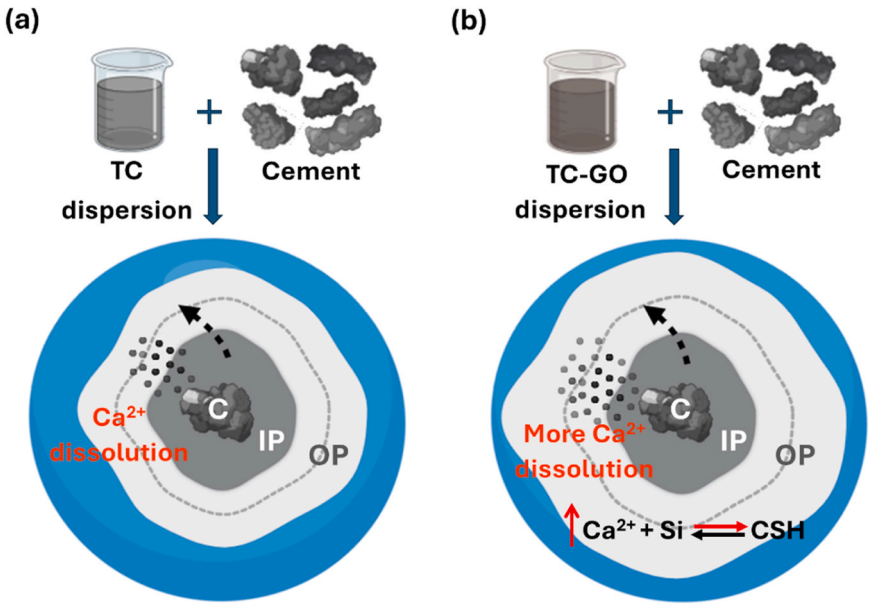

Fig. 14. Schematic representation of the influence mechanism of TC (a) and TC-GO (b) on the formation of cement hydration products.

behavior. While the increase in compressive strength in TC samples is largely due to the thickening of the IP, the lower OP thickness contributes to a reduction in flexural strength, particularly at 0.01 % and 0.05 % TC concentrations. The thinner OP layer in TC samples allows for easier crack propagation during flexural loading, which explains the lower flexural strength compared to control samples.

The compressive strength of TC-GO-added cement mortar gradually increases as the percentage of TC-GO rises, reaching a peak at the optimal dosage. This optimal TC-GO content promotes the formation of a densely packed microstructure. During the cement hydration process, all hydration crystals fully form and bond with the TC-GO sheets. At this point, the compressive strength of the TC-GO-added cement mortar reaches its maximum. However, beyond this optimal dosage, further additions do not enhance compressive strength. This is because all available hydration products have already been incorporated into the dense microstructure, and the additional TC-GO sheets cannot support the formation of fully developed hydration crystals. Instead, partially formed crystal structures emerge. This mechanism explains the reduction in compressive strength when the TC-GO content exceeds the optimal dosage.

Incorporating TC and TC-GO into cement requires a specialised dispersion technique due to the challenges posed by their unique properties. Simply adding TC-GO directly does not yield optimal results, as the sheets tend to agglomerate because of strong Van der Waals forces. This leads to the formation of large clusters, which prevents uniform dispersion in the cement mixture [36]. Additionally, TC-GO particles are hydrophilic due to oxygen functional groups on their surface, they retain some hydrophobic characteristics from the graphene

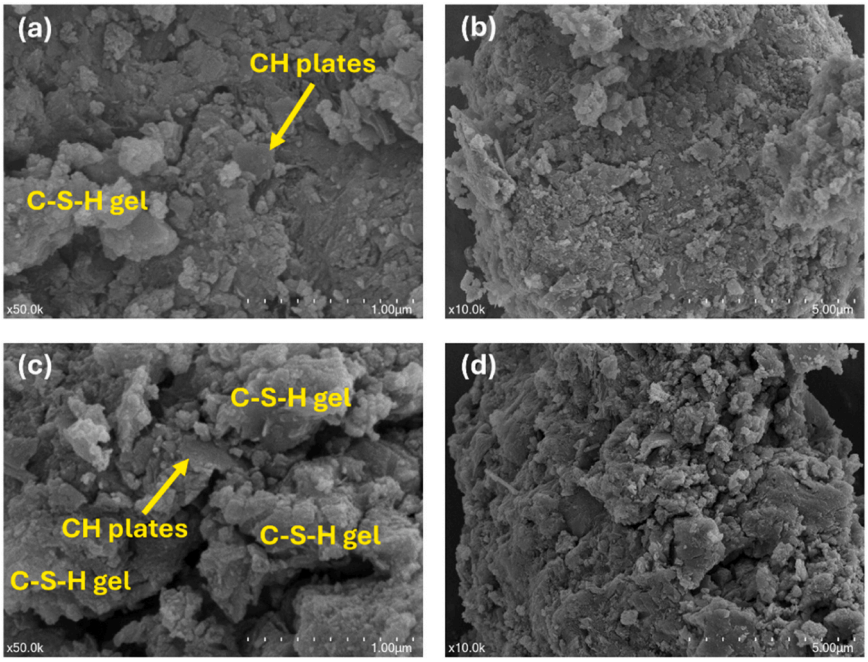

Fig. 15. SEM images of Control (0.00 %) cement mortar (a-b) and TC-GO 0.03 % cement mortar at 28 days (c-d).

structure in TC, further complicating dispersion. Another issue is the high specific area of TC and TC-GO nanoparticles, which increases surface energy and promotes agglomeration. To address these challenges, an ultrasonic mixing technique was used. This method employs high-frequency sound waves to create and collapse microbubbles, generating shock waves and intense shear forces [37]. These forces are more effective than mechanical mixing, breaking down the surface energy between TC and TC-GO sheets at the nanoscale level. With better dispersion, the TC-GO nanoparticles provide more surface area for bonding with cement hydration products, creating numerous nucleation sites. This leads to a denser microstructure and improved strength in the cement [36].

3.5. Microstructural characterisation of TC-GO in cement mortar

The SEM images in Fig. 15 illustrate the microstructure differences between control cement mortar (0.00 %) and TC-GO 0.03 % cement mortar at 28 days. In images (a) and (b), representing the control sample, the microstructure reveals typical cement hydration products, including calcium silicate hydrate (C-S-H) gel and calcium hydroxide (CH) plates [38]. These images highlight a relatively loose and less dense arrangement of hydration products. In contrast, images (c) and (d) of the TC-GO 0.03 % sample show a denser microstructure with more C-S-H and CH plates compared to the control. The finding are consistent with those of Nithurshan et al. [39], who reported that GO incorporation led to the formation of larger C-S-H with folded structures, resulting in reduced porosity and enhanced densification. The presence of TC-GO clearly improves the arrangement of cement hydration products, contributing to a more compact and well-bonded structure. This increased density indicates that TC-GO not only facilitates the formation of more hydration products but also plays a key role in organising the microstructure, leading to better bonding between cement particles. The comparison of the SEM images shows that the TC-GO enhanced sample has fewer voids and a more integrated structure, which likely contributes to improved mechanical properties.

The EDS results and elemetal mapping of the control and 0.03 % TC-GO cement mortar sample, shown in Fig. 16, reveal distinct difference in chemical composition and spatial distribution. Fig. 16 (a-b) presents BSE imaging and EDS mapping of the control sample, which shows a relatively porous microstructure with visible microcracks. The elemental mapping shows strong signals of calcium (Ca), silicon (Si), and oxygen (O), corresponding to the formation of C-S-H gel and portalandite (CH) phases. It should be noted that element H cannot be detected by EDS due to ite very low atomic weight [37]. In contrast, the TC-GO modified sample, shown in Fig. 16 (c-d), exhibits a denser and more complex matrix with fewer visible pores and cracks. The EDS analysis of the TC-GO sample indicates an increased C content, confirming the incorporation of GO. A uniform distribution of C and O in the mapping shows that the GO was well dispersed within the cement matrix. This contrasts with the findings of Suo et al. [40], who reported the presence of GO agglomerates in their elemental maps, indicating less uniform dispersion in their study.

Additionally, a slight reduction in Ca intensity in the TC-GO cement mortar sample indicates reduced CH formation, due to the interaction between GO functional groups and Ca^{2+} ions, which promotes the nucleation of additional C-S-H and refines the micorstructure. This is further supported by a lower Ca/Si ratio of 1.9 in the TC-GO sample compared to 2.4 in the control, suggesting a shift towards C-S-H formation over portalandite. Typically, the Ca/Si ratio of C–S–H varies between 1.5 and 2.5, depending on the hydration conditions and composition. A comparable approach was adopted by Yan et al. [37] who also used the Ca/Si ratio as an indicator to assess the hydration degree in GO-modified cement systems. These findings collectively demonstrate that the addition of TC-GO enhances microstructural uniformity and contributes to improved mechanical performance and durability of the cement mortar.

4. Conclusions

This study introduces an innovative and sustainable approach for enhancing cement mortar by incorporating GO synthesised from TC waste tyre rubber derived char (TC) using two-step MAP process. The synthesis method was used ferric chloride and sulfuric acid, offers cost effective and environmentally friendly alternative to conventional GO production. Structural characterisation using XRD, Raman spectroscopy, XPS and SEM confirmed the successful formation of TC-derived GO (TC-

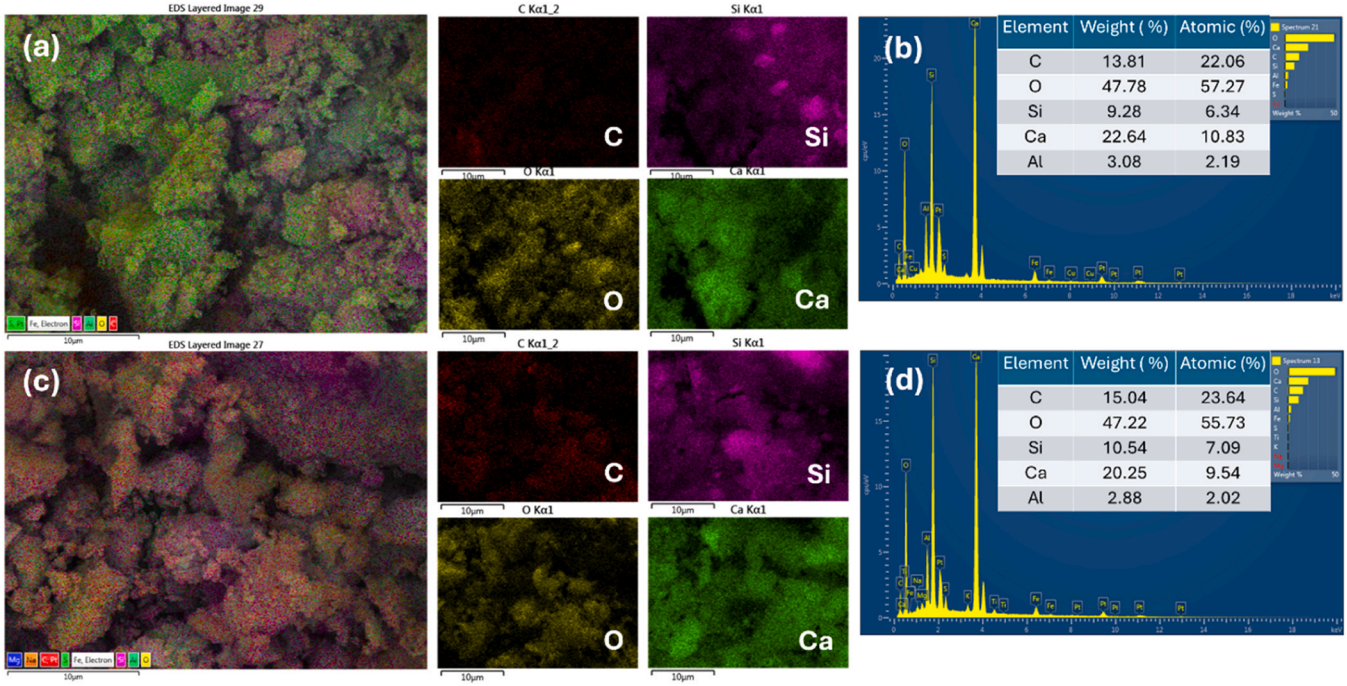

Fig. 16. EDS results and elemetal mapping Control (0.00 %) cement mortar (a-b) and TC-GO 0.03 % cement mortar at 28 days (c-d).

GO). Among the tested dosages, 0.03 % TC-GO exhibited the most significant enhancement in performance, resulting in approximately 15 % higher compressive and flexural strengths at 28 days compared to the control. This improvement was greater than that achieved with 0.03 % TC alone, demonstrating that oxygen-containing functional groups in GO were critical in inducing hydration and improving the microstructure. The use of polycarboxylate superplasticiser was crucial for achieving uniform dispersion of TC-GO. SEM and EDS analyses confirmed a denser matrix and a lower Ca/Si ratio (1.9 vs. 2.4 in control), indicating enhanced C–S–H formation and reduced portlandite. These findings are consistent with previous studies, but more efficient due to the unique synthesis GO process used. TC-GO shows great promise as a cost-effective and sustainable nanomaterial for improving cement-based materials, thereby supporting both material performance and circular economy goals. Future research should explore the scalability of the TC-GO production process, assess long-term durability under various environmental conditions, investigate its integration with other supplementary cementitious materials, and evaluate its influence in concrete and advanced composite systems.

Funding

Chethana received the James Cook University Postgraduate Research Scholarship (JCUPRS). Open-access funding was provided by James Cook University, Townsville, Australia.

CRediT authorship contribution statement

Rabin Tuladhar: Writing – review & editing, Supervision, Project administration, Conceptualization. **Mohan V. Jacob:** Writing – review & editing, Supervision, Project administration, Conceptualization. **Weeraddhana Chethana Himeshani Silva:** Writing – original draft, Methodology, Investigation, Formal analysis, Conceptualization. **Tuan Ngo:** Writing – review & editing, Supervision.

Declaration of Competing Interest

The authors declare that they have no known competing financial interests or personal relationships that could have appeared to influence the work reported in this paper.

Acknowledgement

This research was supported by the James Cook University Postgraduate Research Scholarship (JCUPRS) and the DBI. The author gratefully acknowledges the facilities and technical assistance provided by the Advanced Analytical Centre at James Cook University and the Centre for Microscopy and Microanalysis at The University of Queensland. Sincere appreciation is also extended to the technical staff at James Cook University for their invaluable assistance throughout the project.

Data availability

Data will be made available on request.

References

[1] D. Lu, et al., A targeted approach of using graphene oxide in cement composites, Constr. Build. Mater. 456 (2024) 139339.
[2] K.P. Bautista-Gutierrez, et al., Recent progress in nanomaterials for modern concrete infrastructure: advantages and challenges, Materials 12 (21) (2019) 3548.
[3] J. Li, Q. Zheng, The first experimental evidence for improved nanomechanical properties of calcium silicate hydrate by polycarboxylate ether and graphene oxide, Cem. Concr. Res. 156 (2022) 106787.
[4] L. Zhao, et al., An intensive review on the role of graphene oxide in cement-based materials, Constr. Build. Mater. 241 (2020) 117939.
[5] M.R. Magro, D.A. Vella, G. Cassar, Synthesis of graphene oxide: a refined approach, Carbon Trends 20 (2025) 100509.
[6] J. Yang, et al., The influence of graphene oxide on the hydration and mechanical properties of cement-based materials with low water-binder ratio, Cem. Concr. Compos. 152 (2024) 105640.
[7] Y.W. Yap, et al., Recent advances in synthesis of graphite from agricultural Bio-Waste material: a review, Materials 16 (9) (2023) 3601.
[8] W.C.H. Silva, et al., Sustainable synthesis of graphene oxide from waste sources: a comprehensive review of methods and applications, Mater. Circ. Econ. 6 (1) (2024) 23.
[9] E.H. Sujiono, et al., Graphene oxide based coconut shell waste: synthesis by modified hummers method and characterization, Heliyon 6 (8) (2020) e04568.
[10] B. Thangaraj, et al., Synthesis of graphene oxide from sugarcane dry leaves by Two-Stage pyrolysis, Molecules 28 (8) (2023) 3329.
[11] M.S. Amir Faiz, et al., Preparation and characterization of graphene oxide from tea waste and it's photocatalytic application of TiO2/graphene nanocomposite, Mater. Res. Express 7 (1) (2020) 015613.
[12] K. Singhal, et al., Sustainable development of graphene oxide from pine leaves for electrochemical energy storage and corrosion protection, Curr. Res. Green. Sustain. Chem. 5 (2022) 100266.
[13] M. Fathy, et al., Green synthesis of graphene oxide from oil palm leaves as novel adsorbent for removal of Cu(II) ions from synthetic wastewater, Graph. Technol. 4 (1) (2019) 33–40.
[14] A.U. Anuar, et al., Graphene oxide based regenerated carbon waste tyre (rCB): synthesis by modified hummers method and characterization, Mater. Today. Proc. (2023).
[15] S. Kumar Sahoo, et al., Preparation of graphene oxide from Bio-soot wastes: as an efficient adsorbent for highly noxious Congo red dye, FlatChem 24 (2020) 100198.
[16] A. Loudiki, et al., Graphene oxide synthesized from zinc-carbon battery waste using a new oxidation process assisted sonication: electrochemical properties, Mater. Chem. Phys. 275 (2022) 125308.
[17] R. Roychand, et al., A comprehensive review on the mechanical properties of waste tire rubber concrete, Constr. Build. Mater. 237 (2020) 117651.
[18] P.M. Mayer, et al., Where the rubber meets the road: emerging environmental impacts of tire wear particles and their chemical cocktails, Sci. Total Environ. 927 (2024) 171153.
[19] N. Gao, et al., Tire pyrolysis char: processes, properties, upgrading and applications, Prog. Energy Combust. Sci. 93 (2022) 101022.
[20] C.-Y. Huang, et al., Enhancing cementitious composites with functionalized graphene Oxide-Based materials: surface chemistry and mechanisms, Int. J. Mol. Sci. 24 (13) (2023) 10461.
[21] I. Fonseka, et al., Influence of graphene oxide on abrasion resistance and strength of concrete, Constr. Build. Mater. 404 (2023) 133280.
[22] W.C.H. Silva, et al., Sustainable synthesis and characterisation of tyre Char-Based graphene oxide via Microwave-Assisted pyrolysis, Mater. Circ. Econ. 7 (1) (2025) 26.
[23] General purpose and blended cements, S. Australia, Sydeny, NSW, *2010.*
[24] AS 2350.12–2006 *Methods of testing portland, blended and masonry cements Preparation of a standard mortar and moulding of specimens.*
[25] AS 2701.2001 *Methods of sampling and testing mortar for masonry construction.*
[26] P. Bradder, et al., Dye adsorption on layered graphite oxide, J. Chem. Eng. Data 56 (1) (2011) 138–141.
[27] R. Al-Gaashani, et al., XPS and structural studies of high quality graphene oxide and reduced graphene oxide prepared by different chemical oxidation methods, Ceram. Int. 45 (11) (2019) 14439–14448.
[28] X. Li, et al., Effects of graphene oxide agglomerates on workability, hydration, microstructure and compressive strength of cement paste, Constr. Build. Mater. 145 (2017) 402–410.
[29] Y. Suo, et al., Study on modification mechanism of workability and mechanical properties for graphene oxide-reinforced cement composite, Nanomater. Nanotechnol. 10 (2020) 1847980420912601 (p.).
[30] M. Birenboim, et al., Reinforcement and workability aspects of graphene-oxide-reinforced cement nanocomposites, Composites Part B Engineering 161 (2019) 68–76.
[31] Y. Wang, J. Yang, D. Ouyang, Effect of graphene oxide on mechanical properties of cement mortar and its strengthening mechanism, Materials 12 (22) (2019) 3753.
[32] M. Ullah, et al., Synthesis, characterization and application of graphene oxide in self consolidating cementitious systems, Constr. Build. Mater. 296 (2021) 123623.
[33] D. Cui, et al., Use of graphene oxide to improve the durability and mechanical properties of mortar immersed in flowing river for three years, Nanomaterials 10 (12) (2020) 2385.
[34] E. John, B. Lothenbach, Cement hydration mechanisms through time – a review, J. Mater. Sci. 58 (24) (2023) 9805–9833.
[35] S. Meng, et al., The role of graphene/graphene oxide in cement hydration, Nanotechnol. Rev. 10 (1) (2021) 768–778.
[36] I. Fonseka, et al., Influence of graphene oxide properties, superplasticiser type, and dispersion technique on mechanical performance of graphene oxide-added concrete, Constr. Build. Mater. 428 (2024) 136415.
[37] X. Yan, et al., Study of optimizing graphene oxide dispersion and properties of the resulting cement mortars, Constr. Build. Mater. 257 (2020) 119477.
[38] M. Khawaji, M. Alamri, Potential of enhancing the joint of adjacent cement composites by incorporating edge-oxidized graphene oxide, Case Stud. Constr. Mater. 21 (2024) e03540.
[39] M. Nithurshan, et al., Exploring the reinforcing mechanism of graphene oxide in cementitious materials through microstructural analysis of synthesised calcium silicate hydrate, Cem. Concr. Compos. 153 (2024) 105717.
[40] Y. Suo, et al., Study on self-sensing capabilities of smart cements filled with graphene oxide under dynamic cyclic loading, J. Build. Eng. 58 (2022) 104775.